

# Intensity fluctuations in steady state superradiance

D. Meiser and M. J. Holland

*JILA and Department of Physics, The University of Colorado, Boulder, Colorado 80309-0440, USA*

(Dated: November 17, 2018)

Alkaline-earth like atoms with ultra-narrow optical transitions enable superradiance in steady state. The emitted light promises to have an unprecedented stability with a linewidth as narrow as a few millihertz. In order to evaluate the potential usefulness of this light source as an ultrastable oscillator in clock and precision metrology applications it is crucial to understand the noise properties of this device. In this paper we present a detailed analysis of the intensity fluctuations by means of Monte-Carlo simulations and semi-classical approximations. We find that the light exhibits bunching below threshold, is to a good approximation coherent in the superradiant regime, and is chaotic above the second threshold.

PACS numbers: 42.50.Fx, 37.30.+i, 42.50.Pq, 42.50.Ct, 42.55.Ah, 42.50.Lc

## I. INTRODUCTION

Dicke superradiance is a paradigmatic collective effect in cavity quantum electrodynamics (QED). At the fundamental, level superradiance is a quantum interference effect in which the probability amplitudes for the emission of a photon from several atoms conspire to yield a collective light emission rate that is larger than for uncorrelated atoms. Due to its great conceptual simplicity and generality superradiance has been extensively studied both experimentally and theoretically. The noise properties of the light emitted in superradiance have been of particular interest. This is because the early stages of superradiance are often initiated by quantum fluctuations which are subsequently amplified by the collective emission process [1, 2]. Superradiance can thus serve as a physical phenomenon that allows us to study the microscopic quantum fluctuations through their macroscopic consequences. Examples of this macroscopic manifestation of the quantum fluctuations are the first passage time statistics of the superradiant pulse [3–5] as well as the second order correlations of the field [6].

Nearly all realizations of Dicke superradiance have been in the pulsed regime. In contrast to such experiments we have recently proposed a system based on earth-alkaline-like atoms in which superradiance can be achieved in steady state [7, 8]. The interest in that light source derives from the extremely narrow linewidth of the generated light. For experimentally realizable parameters linewidths in the millihertz range could potentially be realized. The light generated this way could thus serve as an ultra-stable local oscillator with a stability that is about two orders of magnitude better than the current state-of-the-art. At the core of this device are atoms with an ultra-narrow optical transition coupled to a high finesse cavity. The atoms collectively emit photons into the cavity mode and they are concurrently repumped to the excited state, providing a steady supply of energy. The collective decay of the atoms via the cavity mode establishes a collective atomic dipole, which radiates much more strongly than independent atoms would. Depending on the repumping rate, the system can also exhibit

subradiance, or thermal light as would be the case for an ensemble of random radiators. Qualitatively similar behavior has been predicted for the overdamped many-atom micromaser [9].

Just as for pulsed Dicke superradiance, the higher order correlations of the light are non-trivial and a solid knowledge of them is crucial for a full understanding of the collective light generation mechanism as well as for potential applications. Correlations of the intensity can be used to quantitatively study these fluctuations and these are the subject of this paper. Some aspects of the noise properties of continuously pumped, collectively emitting systems have also been discussed recently in the context of collectively radiating low dimensional solid state systems [10, 11]. For instance Temnov and Woggon studied the photon statistics deep in the subradiant regime in [12].

The goal of this paper is to fully characterize the intensity correlations of the light generated by means of steady state superradiance. To this end we introduce a simplified model that captures all the essential aspects of the problem in section II and we recall the basics of steady state superradiance. Section III presents our results on the Hanbury Brown-Twiss correlations of the generated light obtained for small atom numbers using quantum Monte-Carlo simulations and semiclassical approximations in the limit of large atom numbers.

## II. MODEL

Calculating higher order correlations of quantum fields is typically a hard problem. Analytic closed form solutions are known in only a few special cases and thus we have to rely mostly on numerical simulations. Because of the exponential scaling of the dimension of the Hilbert space of the system with the number of atoms we must restrict ourselves to the simplest model that still captures the essential physics that we are interested in.

The core ingredients of a system exhibiting steady state superradiance are illustrated in Fig. 1. An ensemble of  $N$  two level atoms with excited state  $|e\rangle$ , ground

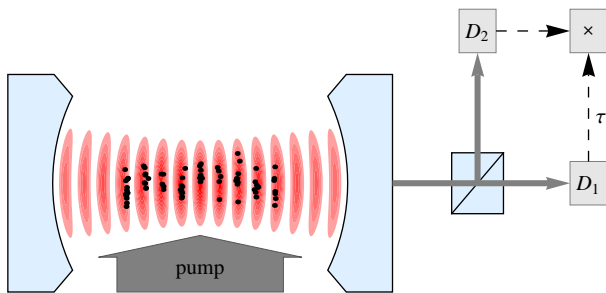


FIG. 1: (Color online) Schematic illustration of  $N$  two level atoms confined in a single mode cavity field indicated by the black dots. The atoms are being incoherently repumped. The output of the cavity field is monitored by two detectors  $D_1$  and  $D_2$  with a variable time delay  $\tau$  between them.

state  $|g\rangle$ , and transition frequency  $\omega_a$  are collectively coupled to a high finesse cavity with resonance frequency  $\omega_c$ . The atoms are independently repumped from the ground state to the excited state in order for the atoms to be able to radiate photons continuously.

The non-collective nature of the repumping is essential for two reasons. First, it is much easier to achieve experimentally than collective repumping, for instance by optical pumping through an auxiliary excited state. Second, and somewhat paradoxically, it can balance the effects of other incoherent processes such as spontaneous emission and dephasing that would normally drive the atoms into less collective states that do not exhibit superradiance. A purely collective repumping as considered e.g. in [13, 14] cannot change the length of the atomic Bloch vector. Therefore, if the length decays due to dissipative processes, it cannot be restored and the superradiance stops. In contrast, the length of the atomic Bloch vector can grow in the case of non-collective pumping so that a collective atomic dipole can develop from an ensemble of completely independent atoms.

### A. Atom-field master equation

Mathematically, the coupled atom cavity system can be described by the Hamiltonian

$$\hat{H} = \hbar\omega_a \hat{J}_z + \hbar\omega_c \hat{a}^\dagger \hat{a} + \frac{\hbar g}{2} (\hat{a}^\dagger \hat{J}_- + \hat{J}_+ \hat{a}). \quad (1)$$

Here we have introduced an angular momentum representation for the atoms in the usual way by identifying the excited state with the spin up state of a fictitious spin 1/2 system and the ground state with the spin down state. The operators

$$\hat{J}_z = \frac{1}{2} \sum_{j=1}^N \hat{\sigma}_z^{(j)} \quad (2)$$

and

$$\hat{J}_- = \hat{J}_+^\dagger = \sum_{j=1}^N \hat{\sigma}_-^{(j)} \quad (3)$$

are the  $z$ -component and ladder operators of the total angular momentum. In these equations  $\hat{\sigma}_z^{(j)} = |e\rangle\langle e| - |g\rangle\langle g|$  is a Pauli matrix pertaining to atom number  $j$  and  $\hat{\sigma}_- = \hat{\sigma}_+^\dagger = |g\rangle\langle e|$  is the spin-flip operator for atom  $j$ . The operators  $\hat{a}$  and  $\hat{a}^\dagger$  are the annihilation and creation operators for a photon in the cavity mode. For simplicity we assume that the coupling constant  $g$  of the atoms to the cavity is identical for all atoms. This could, in principle, be achieved by trapping the atoms at the antinodes of the cavity mode. Less ideal spatial configurations of the atoms merely lead to a reduction of the effective number of atoms by a factor of order one that clearly has no impact on the basic conclusions of this paper.

Besides the coherent interaction of the atoms with the cavity field there are also dissipative processes due to the coupling of the atoms to field modes outside of the cavity and due to decay of the cavity fields. The decay of the cavity can be accounted for with the usual Born-Markov master equation for the reduced density matrix for atoms and cavity field,

$$\frac{d\hat{\rho}}{dt} = \frac{1}{i\hbar} [\hat{\rho}, \hat{H}] + \mathcal{L}_{\text{cav}}[\hat{\rho}] + \mathcal{L}_{\text{pump}}[\hat{\rho}], \quad (4)$$

where the Liouvillian for the cavity decay with intensity decay rate  $\kappa$  is

$$\mathcal{L}_{\text{cav}}[\hat{\rho}] = -\frac{\kappa}{2} (\hat{a}^\dagger \hat{a} \hat{\rho} + \hat{\rho} \hat{a}^\dagger \hat{a} - 2\hat{\rho} \hat{a} \hat{a}^\dagger). \quad (5)$$

The repumping of the atoms with pump rate  $w$  is described by the Liouvillian

$$\mathcal{L}_{\text{pump}}[\hat{\rho}] = -\frac{w}{2} \sum_{j=1}^N (\hat{\sigma}_-^{(j)} \hat{\sigma}_+^{(j)} \hat{\rho} + \hat{\rho} \hat{\sigma}_-^{(j)} \hat{\sigma}_+^{(j)} - 2\hat{\sigma}_+^{(j)} \hat{\rho} \hat{\sigma}_-^{(j)}). \quad (6)$$

We are assuming that the spontaneous emission of the atoms into free space with decay rate  $\gamma$  can be neglected. In general this assumption requires  $\mathcal{C} \gg 1$  where  $\mathcal{C} = g^2/(\kappa\gamma)$  is the single atom cooperativity parameter, see Eq. (8) below. Note however that in the superradiant regime where the decay through the cavity is collectively enhanced it is found that the much less stringent condition  $N\mathcal{C} \gg 1$  is sufficient for this approximation to be justified.

In order to calculate correlation functions of the generated light field we simulate the dynamics of the system subject to the master equation (4) using the Monte-Carlo wavefunction technique [15–17]. In that technique the evolution of the system is represented by an ensemble of stochastic wavefunction trajectories  $\{|\psi(t)\rangle\}$  where each trajectory  $|\psi(t)\rangle$  is a representative evolution of the system.

## B. Adiabatic elimination of field in “bad cavity” limit

The Hamiltonian Eq. (1) is suitable for the Monte-Carlo simulations because it directly grants access to the field correlations we are interested in. For analytical calculations it is desirable to further simplify the problem by exploiting the fact that the cavity field decays so much faster than the atomic coherence. Adiabatically eliminating the light field yields the effective superradiance master equation [6],

$$\begin{aligned} \frac{d\hat{\rho}}{dt} = & -\frac{\Gamma_c}{2} \left( \hat{J}_+ \hat{J}_- \hat{\rho} + \hat{\rho} \hat{J}_+ \hat{J}_- - 2\hat{J}_- \hat{\rho} \hat{J}_+ \right) \\ & - \frac{w}{2} \sum_{j=1}^N \left( \hat{\sigma}_-^{(j)} \hat{\sigma}_+^{(j)} \hat{\rho} + \hat{\rho} \hat{\sigma}_-^{(j)} \hat{\sigma}_+^{(j)} - 2\hat{\sigma}_+^{(j)} \hat{\rho} \hat{\sigma}_-^{(j)} \right). \end{aligned} \quad (7)$$

Here, the collective decay rate of the atoms is given by

$$\Gamma_c = \mathcal{C}\gamma = g^2/\kappa. \quad (8)$$

The condition for the validity of the adiabatic elimination of the cavity field is that the cavity field relaxes much faster as the atoms. Using that the fastest atomic relaxation rates are obtained in the superradiant regime and that they are of order  $N\mathcal{C}\gamma$  we find the quantitative condition

$$\kappa \gg N\mathcal{C}\gamma. \quad (9)$$

In this “bad cavity” limit the role of the cavity mode reduces to providing a collective decay channel for the atoms. The simplification brought about by the elimination of the field is two-fold. It allows us to deal with the atomic degrees of freedom only and all parameters of the full coupled atom-cavity system have collapsed into just one characteristic parameter,  $w/\Gamma_c$ .

## C. Hanbury-Brown-Twiss signal

Fluctuations of the light intensity can be characterized experimentally by a Hanbury-Brown-Twiss-like setup as illustrated in Fig. 1 [18, 19]. The light passes through a 50/50 beam splitter and the intensities in each output-port of the beam-splitter is detected with a photo-diode. The photo-currents of each detector are then multiplied and integrated. A variable delay  $\tau$  can be imparted on one of the outputs of the beam splitter in order to measure correlations of the field at different times. Using such a setup it is possible to measure the joint probability  $P_2(t, t+\tau)\Delta t\Delta\tau$  to detect a photon both in a time interval  $\Delta t$  at  $t$  and in a time interval  $\Delta\tau$  at  $t+\tau$ . According to the theory of photo-detection [19, 20] this probability can be calculated in terms of normally ordered expecta-

tion values of the field amplitude,

$$\begin{aligned} g^{(2)}(t, \tau) &\equiv \frac{P_2(t, t+\tau)\Delta t\Delta\tau}{P_1(t)\Delta t P_1(t+\tau)\Delta\tau} \\ &= \frac{\langle \hat{a}^\dagger(t)\hat{a}^\dagger(t+\tau)\hat{a}(t+\tau)\hat{a}(t) \rangle}{\langle \hat{a}^\dagger(t)\hat{a}(t) \rangle \langle \hat{a}^\dagger(t+\tau)\hat{a}(t+\tau) \rangle}. \end{aligned} \quad (10)$$

We have normalized the joint probability to the single time probabilities for photon detection,  $P_1(t)\Delta t$  and  $P_1(t+\Delta\tau)\Delta\tau$ . In steady state, which is the case of primary interest here,  $g^{(2)}(t, \tau)$  does not depend on  $t$ . For notational convenience we drop the variable  $t$  from  $g^{(2)}(t, \tau)$ , i.e. we simply write  $g^{(2)}(\tau)$ . In writing Eq. (10) we have also made use of the result from the input-output theory for cavities that normally ordered correlation functions outside of a cavity are equal to the normally ordered correlation functions of the intra-cavity field, provided that the input ports of the cavity are in vacuum states [21, 22].

The second order correlation function at zero time delay,  $g^{(2)}(0)$ , is related to the fluctuations  $\Delta I^2 = \langle \hat{I}^2 \rangle - \langle \hat{I} \rangle^2$  of the out-coupled photon flux  $\hat{I}$ . These fluctuations  $\Delta I^2$  can be used to characterize the instability of the intensity of the out-coupled beam because  $\hat{I}$  is proportional to the beam intensity. Typical photo detectors have a detection bandwidth  $B$  that is extremely large compared to the cavity bandwidth and in that case the fluctuations of the intensity are given by

$$\Delta I^2 = I^2(g^{(2)}(0) - 1) + BI, \quad (11)$$

where  $I = \langle \hat{I} \rangle$ . For coherent light the arrival of photons at the detectors are a Poisson process in which the arrival times are completely random with mean rate of arrival  $I$ . For such light  $\Delta I^2 = BI$  and we have  $g^{(2)}(0) = 1$ . Light with larger intensity fluctuations is called super-Poissonian and light with smaller intensity fluctuations is called sub-Poissonian. Super-Poissonian light has  $g^{(2)}(0) > 1$  and photons arrive in bunches, while sub-Poissonian light has  $g^{(2)} < 1$  and photons are anti-bunched, i.e. they arrive more regularly than predicted by Poisson statistics.

Our numerical wave-function Monte-Carlo simulations grant us access to correlation functions in two ways. First, we can calculate expectation values of *system* observables  $\hat{O}$  in the usual way by calculating  $\langle \psi | \hat{O} | \psi \rangle$  and averaging over the ensemble of trajectories. Alternatively we can extract the correlation functions by an analysis of the decay times of the system that very closely mirrors an actual experimental procedure. This latter method is easier to implement for non-zero time delays. All results on the intensity correlations presented here were calculated this way due to the greater flexibility of having access to zero and non-zero delays.

The procedure by which we calculate  $g^{(2)}(\tau)$  from the cavity decay times is illustrated in Fig. 2. Part a) of that figure shows the evolution of the mean photon number inside the cavity for an example trajectory. Cavity decay events are indicated by the black ticks at times  $t_i$ . For

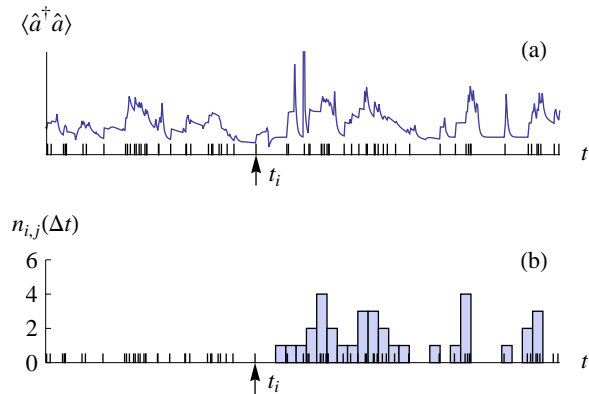


FIG. 2: (Color online) Time evolution of the intracavity intensity during a single Monte-Carlo trajectory (a) for  $N = 10$  atoms and  $w = 5\Gamma_c$ . The black ticks indicate cavity decay events. Panel (b) shows the binning of the decay times subsequent to  $t_i$  leading to the histogram  $n_{i,j}(\Delta t)$  used in the calculation of  $g^{(2)}(\tau)$  (see text for explanation).

each photon emission event we calculate the Histogram  $n_{i,j}(\Delta t) = \# \text{photons in } (t_i + j\Delta t, t_i + (j+1)\Delta t]$ . By averaging these histograms over all  $i$  we find  $\bar{n}_j(\Delta t) = n_{\text{phot}}^{-1} \sum_i n_{i,j}(\Delta t)$ , where  $n_{\text{phot}}$  is the total number of photons emitted. This histogram is closely related to the conditional probability  $P(t+j\Delta t|t)$  to find a second photon at time  $t+j\Delta t$  provided that a first photon has been detected at time  $t$ , *i.e.*  $\bar{n}_j(\Delta t) = \Delta t P(t+j\Delta t|t)$ . Using the relation between that conditional probability and the joint probability,  $P_2(t, t+j\Delta t) = P(t+j\Delta t|t)P_1(t)$ , we can then find  $g^{(2)}(j\Delta t)$  on a grid with spacing  $\Delta t$  according to

$$g^{(2)}(j\Delta t) = \frac{\bar{n}_j(\Delta t)}{n_{\text{phot}}/\#\text{bins}}, \quad (12)$$

where  $n_{\text{phot}}/\#\text{bins} = P_1(t)\Delta t$  is the mean number of photons per bin. The choice of the bin width  $\Delta t$  is a trade off between resolution and statistical fluctuations and it has to be chosen differently for different simulation parameters. It must be small enough to resolve the dynamics of the system. Once that constraint is satisfied it should be as long as possible in order to yield the smallest fluctuations.

### III. RESULTS

Generally, as explained in detail in [8], three regimes of light emission can be distinguished depending on the repump strength. If the repump rate is smaller than the effective atomic decay rate,  $w \ll \Gamma_c$ , the atoms evolve into a dark state in which the emission of photons is strongly suppressed despite nearly half the atoms being in the excited state. In the intermediate regime,  $\Gamma_c < w < N\Gamma_c$ , the atoms emit light in a superradiant fashion

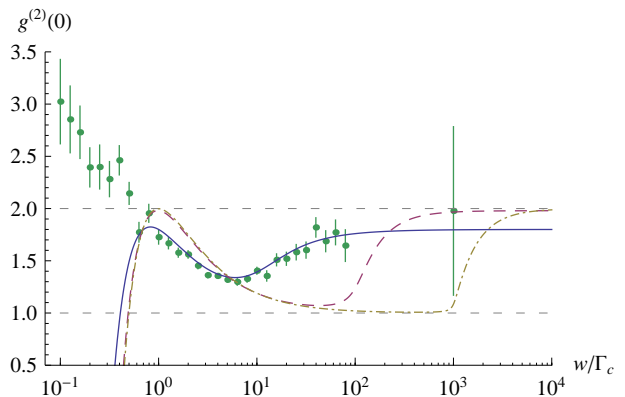


FIG. 3: (Color online) Second order intensity correlation  $g^{(2)}(0)$  as a function of the repump rate. The green symbols show the Monte-Carlo results including the statistical errors for  $N = 10$  atoms. The blue solid line shows the analytical result Eq. (17) for  $N = 10$  atoms, the purple dashed line is for  $N = 100$  atoms, and the yellow dash-dotted line is for  $N = 1000$  atoms. The gray dashed lines at  $g^{(2)}(0) = 2$  and  $g^{(2)}(0) = 1$  are for orientation.

and in the strong pumping limit,  $w \gg N\Gamma_c$ , nearly all atoms are in the excited state and they emit chaotic light like an ensemble of thermally excited atoms.

#### A. Monte-Carlo results for $g^{(2)}(0)$

First we consider  $g^{(2)}(0)$  shown in Fig. 3 for  $N = 10$  atoms. The error bars in that figure are estimates of the statistical uncertainty obtained by treating the histograms  $n_{i,j}(\Delta t)$  for different  $i$  as independent of each other.

In the weak pumping limit the light exhibits strongly super-Poissonian fluctuations indicating photon bunching. This bunching effect can easily be understood in the extreme limit  $w/\Gamma_c \rightarrow 0$  [8, 12]. In that limit the atoms are optically pumped into collective dark states [23, 24]  $|J = 1, M = -1\rangle$  and  $|J = 0, M = 0\rangle$  [26]. From  $|J = 0, M = 0\rangle$  the atoms can only be pumped to  $|J = 1, M = 1\rangle$  from which they relax to  $|J = 1, M = -1\rangle$  by rapidly emitting a pair of photons in a cascade within a time of order  $\Gamma_c^{-1}$ .

In the superradiant regime for intermediate pumping  $g^{(2)}(0)$  is reduced to a value about half way between 1 and 2. It reaches a minimum at the superradiant emission maximum,  $w = N\Gamma_c/2$ . The minimum value depends on  $N$  with larger  $N$  yielding smaller  $g^{(2)}(0)$ .

In the limit of very strong repumping the atoms behave like a thermal ensemble of atoms. Therefore we have  $g^{(2)}(0) = 2(1-1/N)$  in that limit in very good agreement with the Monte-Carlo simulation results.

## B. Semi-classical results for $g^{(2)}(0)$

In applications, the number of atoms will typically be much larger than 1. That makes it easier to achieve the collective strong coupling regime where  $N\mathcal{C} \gg 1$ . Furthermore, the collective nature of the light emission is more apparent in that limit.

Unfortunately, the Monte-Carlo simulations on which the above results were based, cannot be easily implemented for the study of large atom numbers. The reason for this is that the size of the system Hilbert space,  $d = 2^N$ , scales exponentially with the number of atoms. In this section, in order to bypass these difficulties, we exploit the possibility for a semiclassical approximation that precisely derives from the largeness of  $N$ . The key idea is that in a macroscopic ensemble of atoms the correlations between  $n$  atoms can be expressed in terms of the correlations between  $n - 1$  atoms plus an error term. Ordinarily, the error terms become smaller as the “cluster size”  $n$  is increased. The approximate treatment that we employ here assumes that correlations between more than two atoms can be completely expressed in terms of pair correlations and single atom quantities.

The semi-classical calculation involves two non-trivial steps. First we have to find the correlations between the spins of different atoms. Second we have to find an expression for  $g^{(2)}(0)$  in terms of the atomic correlations.

### 1. Steady state solutions for pair correlations

The symmetry of the expectation values with respect to particle exchange greatly reduces the number of expectation values that have to be considered. We have for instance  $\langle \hat{\sigma}_+^{(i)} \hat{\sigma}_-^{(j)} \rangle = \langle \hat{\sigma}_+^{(1)} \hat{\sigma}_-^{(2)} \rangle$  for all  $i \neq j$ . Up to the level of pair correlations, all observables that we are interested in can be expressed in terms of  $\langle \hat{\sigma}_z^{(1)} \rangle$ ,  $\langle \hat{\sigma}_+^{(1)} \hat{\sigma}_-^{(2)} \rangle$ , and  $\langle \hat{\sigma}_z^{(1)} \hat{\sigma}_z^{(2)} \rangle$ .

The equations of motion for these expectation values can be found from the master equation (7),

$$\frac{d\langle \hat{\sigma}_z^{(1)} \rangle}{dt} = -(w + \Gamma_c) \left( \langle \hat{\sigma}_z^{(1)} \rangle - d_0 \right) - 2\Gamma_c(N - 1) \langle \hat{\sigma}_+^{(1)} \hat{\sigma}_-^{(2)} \rangle, \quad (13)$$

where  $d_0 = (w - \Gamma_c)/(w + \Gamma_c)$ ,

$$\begin{aligned} \frac{d\langle \hat{\sigma}_+^{(1)} \hat{\sigma}_-^{(2)} \rangle}{dt} &= -(w + \Gamma_c) \langle \hat{\sigma}_+^{(1)} \hat{\sigma}_-^{(2)} \rangle \\ &+ \frac{\Gamma_c}{2} \left( \langle \hat{\sigma}_z^{(1)} \hat{\sigma}_z^{(2)} \rangle + \langle \hat{\sigma}_z^{(1)} \rangle \right) \\ &+ \Gamma_c(N - 2) \langle \hat{\sigma}_z^{(1)} \hat{\sigma}_+^{(2)} \hat{\sigma}_-^{(3)} \rangle, \end{aligned} \quad (14)$$

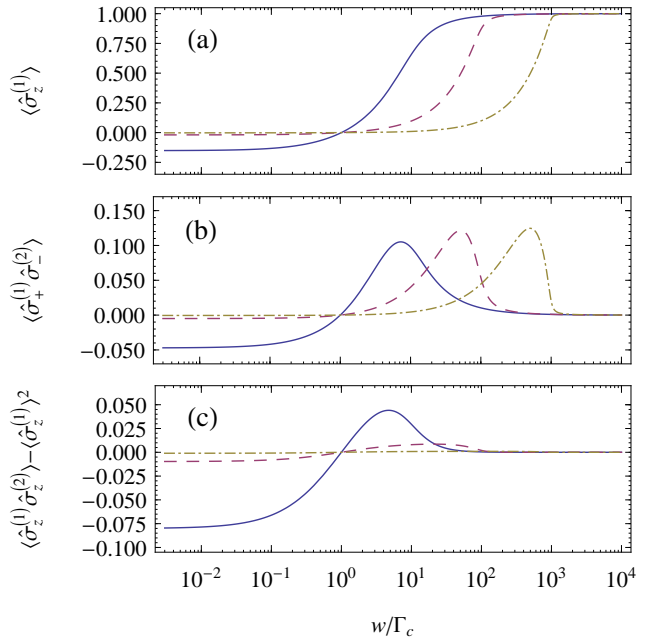


FIG. 4: (Color online) (a) Inversion  $\langle \hat{\sigma}_z^{(1)} \rangle$ , (b) spin-spin correlation  $\langle \hat{\sigma}_+^{(1)} \hat{\sigma}_-^{(2)} \rangle$ , and (c) spin-spin correlation  $\langle \hat{\sigma}_z^{(1)} \hat{\sigma}_z^{(2)} \rangle - \langle \hat{\sigma}_z^{(1)} \rangle^2$  as a function of pump strength for  $N = 10$  (blue solid line),  $N = 100$  (purple dashed line), and  $N = 1000$  atoms (yellow dash-dotted line).

and

$$\begin{aligned} \frac{d\langle \hat{\sigma}_z^{(1)} \hat{\sigma}_z^{(2)} \rangle}{dt} &= -2(w + \Gamma_c) \left( \langle \hat{\sigma}_z^{(1)} \hat{\sigma}_z^{(2)} \rangle - d_0 \langle \hat{\sigma}_z^{(1)} \rangle \right) \\ &+ 4\Gamma_c \left( \langle \hat{\sigma}_+^{(1)} \hat{\sigma}_-^{(2)} \rangle \right. \\ &\quad \left. - (N - 2) \langle \hat{\sigma}_z^{(1)} \hat{\sigma}_+^{(2)} \hat{\sigma}_-^{(3)} \rangle \right). \end{aligned} \quad (15)$$

We have checked that the third order expectation values  $\langle \hat{\sigma}_z^{(1)} \hat{\sigma}_+^{(2)} \hat{\sigma}_-^{(3)} \rangle$  can be factorized according to

$$\langle \hat{\sigma}_z^{(1)} \hat{\sigma}_+^{(2)} \hat{\sigma}_-^{(3)} \rangle \approx \langle \hat{\sigma}_z^{(1)} \rangle \langle \hat{\sigma}_+^{(1)} \hat{\sigma}_-^{(2)} \rangle$$

to a very good approximation by evaluating them in our Monte-Carlo simulations and by approximating them in terms of lower order cumulants in the adiabatic approximation. By factorizing this way we obtain a closed set of equations. The steady state expectation values are obtained by setting the time derivatives equal to zero. The resulting algebraic equations can be solved analytically for  $\langle \hat{\sigma}_z^{(1)} \rangle$ ,  $\langle \hat{\sigma}_+^{(1)} \hat{\sigma}_-^{(2)} \rangle$ , and  $\langle \hat{\sigma}_z^{(1)} \hat{\sigma}_z^{(2)} \rangle$ , leading to relatively complicated expressions that we reproduce in the appendix for completeness. Plots of the steady state expectation values are given in Fig. 4 for different atom numbers. For large atom numbers the inversion  $\langle \hat{\sigma}_z \rangle$  is essentially zero below threshold for collective emission, increases linearly with  $w$  in the superradiant regime, and saturates with all atoms in the excited state in the strong

pumping regime. In the superradiant regime, the spin-spin correlation  $\langle \hat{\sigma}_+^{(1)} \hat{\sigma}_-^{(2)} \rangle$  is approximately described by an inverted parabola with zeros at the thresholds  $w = \Gamma_c$  and  $w = N\Gamma_c$  and a peak value of  $1/8$  at  $w = N\Gamma_c/2$ . In the strong pumping regime these correlations are destroyed by the repumping. The spin-spin correlations  $\langle \hat{\sigma}_z^{(1)} \hat{\sigma}_z^{(2)} \rangle$  approximately factorize as  $\langle \hat{\sigma}_z^{(1)} \hat{\sigma}_z^{(2)} \rangle \approx \langle \hat{\sigma}_z^{(1)} \rangle^2$  in the limit of large atom numbers. Note that the equations for  $\langle \hat{\sigma}_z^{(1)} \rangle$  and  $\langle \hat{\sigma}_+^{(1)} \hat{\sigma}_-^{(2)} \rangle$  close if that factorization is made and consequently much simpler approximate expressions can be obtained for  $w > \Gamma_c$  in the limit  $N \rightarrow \infty$  as pointed out in [8]. However, since we would like to compare the semi-classical theory with the Monte-Carlo results that were obtained for only relatively small atom numbers, we have to use the more complicated expressions discussed here.

## 2. Expression of $g^{(2)}(0)$ in terms of atomic operators in the bad cavity limit

In the bad cavity limit discussed in subsection II B the cavity field is slaved to the atomic dipoles,

$$\hat{a} \cong \frac{g}{i\kappa} \hat{J}_- . \quad (16)$$

This means that we can calculate correlation functions of the field if we know atomic correlation functions, for instance

$$\begin{aligned} g^{(2)}(0) &= \frac{\langle \hat{J}_+ \hat{J}_+ \hat{J}_- \hat{J}_- \rangle}{\langle \hat{J}_+ \hat{J}_- \rangle^2} \\ &= \frac{\sum_{i,j,k,l=1}^N \langle \hat{\sigma}_+^{(i)} \hat{\sigma}_+^{(j)} \hat{\sigma}_-^{(k)} \hat{\sigma}_-^{(l)} \rangle}{\left( \sum_{i,j=1}^N \langle \hat{\sigma}_+^{(i)} \hat{\sigma}_-^{(j)} \rangle \right)^2} . \end{aligned} \quad (17)$$

The atomic expectation values can be expressed in terms of the above expectation values,

$$\sum_{i,j=1}^N \langle \hat{\sigma}_+^{(i)} \hat{\sigma}_-^{(j)} \rangle = N(\langle \hat{\sigma}_z^{(1)} \rangle + 1)/2 + N(N-1)\langle \hat{\sigma}_+^{(1)} \hat{\sigma}_-^{(2)} \rangle , \quad (18)$$

and

$$\begin{aligned} \langle \hat{J}_+ \hat{J}_+ \hat{J}_- \hat{J}_- \rangle &= N(N-1) \\ &\times \left( 2(N-2)(\langle \hat{\sigma}_z^{(1)} \rangle + 1)\langle \hat{\sigma}_+^{(1)} \hat{\sigma}_-^{(2)} \rangle \right. \\ &\quad + (1 + \langle \hat{\sigma}_z^{(1)} \hat{\sigma}_z^{(2)} \rangle + 2\langle \hat{\sigma}_z^{(1)} \rangle^2)/2 \\ &\quad \left. + (N-2)(N-3)\langle \hat{\sigma}_+^{(1)} \hat{\sigma}_-^{(2)} \rangle^2 \right) . \end{aligned} \quad (19)$$

In order to arrive at this last result we have factorized expectation values for four different atoms according to  $\langle \hat{\sigma}_+^{(1)} \hat{\sigma}_+^{(2)} \hat{\sigma}_-^{(3)} \hat{\sigma}_-^{(4)} \rangle \approx \langle \hat{\sigma}_+^{(1)} \hat{\sigma}_-^{(2)} \rangle^2$ . Expectation values in which at least two indices are identical involve at most three different atoms and, with the factorization discussed earlier, they reduce to the known pair correlations and single atom expectation values.

## 3. Comparison with Monte-Carlo results

The semi-classical results for  $g^{(2)}(0)$  are also shown in Fig. 3. The semi-classical curve agrees very well with the Monte-Carlo results for  $w > \Gamma_c$ . Below that threshold the semi-classical expression yields unphysical values. The disagreement below threshold is not surprising because the atoms are in a very highly correlated state in that regime and these correlations cannot be captured by taking into account only pair-wise correlations.

The good agreement between semi-classical and Monte-Carlo results for  $w > \Gamma_c$  allows us to use the semi-classical expression to extrapolate to very large atom numbers. We find that for large atom numbers the field exhibits nearly coherent counting statistics, *i.e.*  $g^{(2)}(0) \approx 1$ , in the superradiant regime,  $\Gamma_c \ll w < N\Gamma_c$ , and it has the counting statistics of chaotic light in the strong pumping regime.

## C. Monte-Carlo results for $g^{(2)}(\tau)$

The correlations between photons arriving at a photodetector characterized by  $g^{(2)}(0)$  only persist for a certain amount of time. To study the decay of these intensity correlations we show the second order correlation for non-zero delay,  $\tau \neq 0$ , for 10 atoms in Fig. 5.

The strong bunching peak in the subradiant regime decays on a time scale of order  $\Gamma_c^{-1}$  [12]. After that an anti-correlation dip develops for a period of order  $\sim w^{-1}$  because the repumping has to take the system out of the dark states before another photon can be emitted.

In the superradiant regime the bunching is much weaker. The bunching peak also disappears on a much shorter time scale of order  $\sim 1/(N\Gamma_c)$ . The subsequent anti-correlation is a much weaker effect that disappears as  $1/N$  in the limit of large atom numbers. For times  $\tau \gg w^{-1}, (N\Gamma_c)^{-1}$  the light intensities are uncorrelated. This is remarkable because the *amplitude* of the field is coherent for much longer times of order  $\Gamma_c^{-1}$ . Intensity correlations decay on a time scale set by the collective decay of the system while the decay of the amplitude correlations occurs on the time scale set by the single particle decay. From the perspective of potential applications of this light source as an ultra-stable local oscillator this means that the field can be considered as coherent to a very good approximation.

As pointed out above the atoms behave like a thermal ensemble in the strong pumping regime. The two-time correlation function agrees well with the result for thermal light emitted by a large number of atoms [25],

$$g^{(2)}(t) \approx 1 + |g^{(1)}(\tau)|^2 \approx 1 + e^{-\frac{2t}{w}} . \quad (20)$$

The slight discrepancy between this formula and the numerical results is likely due to the relatively small number of atoms considered while Eq.(20) is derived in the limit  $N \rightarrow \infty$ .

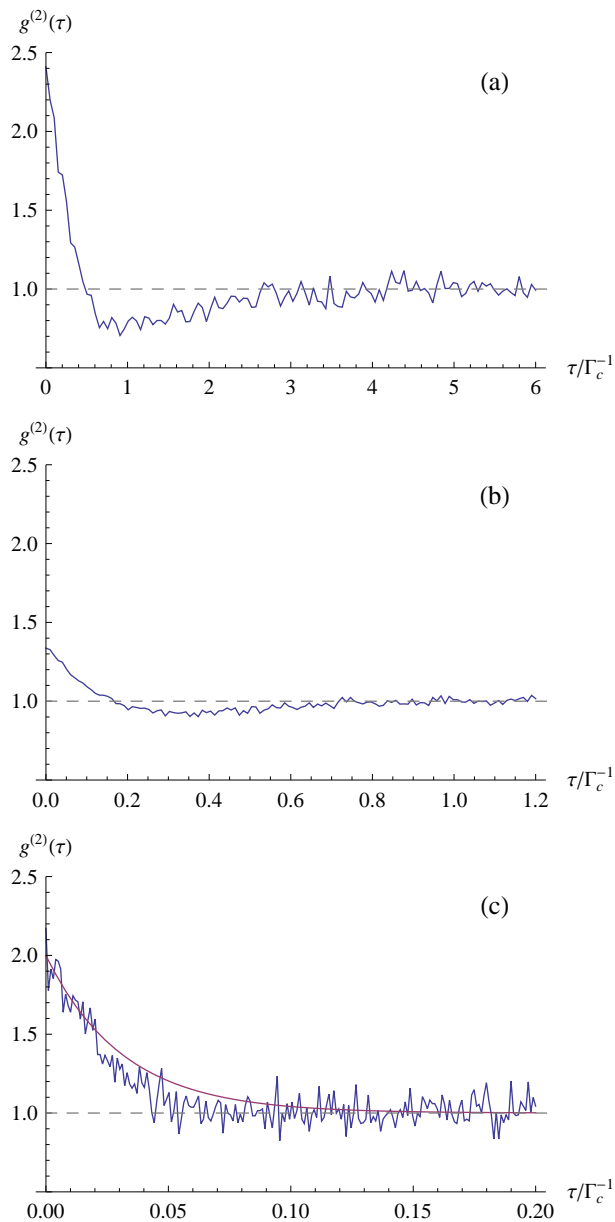


FIG. 5: (Color online) Second order correlation  $g^{(2)}(\tau)$  for  $N = 10$  atoms (a) for the subradiant regime for weak pumping  $w = 0.25\Gamma_c$ , (b) for the superradiant regime with  $w = 5.0\Gamma_c$ , and (c) for the strong pumping regime with  $w = 100\Gamma_c$ . Note the different scales on the time axis for each figure. The purple line in (c) is the thermal light result.

#### IV. CONCLUSION

The key result of this paper is that the light emitted in steady state superradiance is second order coherent in the limit of large atom numbers. This result is significant because it establishes that the coherence properties of the emitted light are closer to those of a laser than those of light generated in ordinary pulsed superradiance. In contrast, light generated in pulsed superradiance would have super-Poissonian intensity fluctuations.

Such excess fluctuations could adversely affect the utility of light sources based on steady state superradiance as a stable frequency reference, one of the main motivations for studying this system in the first place. For such applications it is crucial that the long coherence time and collectively enhanced brightness demonstrated previously [7] are paired with small intensity fluctuations.

In the subradiant regime the emitted light exhibits strong bunching and super-Poissonian intensity fluctuations. As has been pointed out previously by Temnov and Woggon [12] this effect could be useful in identifying and analyzing the subradiant regime in experiment. The well understood thermal character of the atomic ensemble in the strong pumping regime serves as a valuable benchmark for the validity of our theoretical treatment.

In future research we plan to systematically investigate the cross-over from steady state superradiance to a laser. In the extreme limits of this cross-over the system is dominated by purely atomic collective enhancement on the one hand and by purely photonic collective enhancement through stimulated emission on the other hand. The intermediate regime between the two where both collective enhancement due to stimulated emission and an atomic collective state are equally important is very intriguing from a fundamental point of view.

#### Acknowledgments

We are grateful for stimulating discussions with J. K. Thompson, Jun Ye, and J. Cooper. This work has been supported by NSF and ARO.

#### Appendix A: Steady-state atomic pair correlations

In this appendix we summarize the analytical solution of the semi-classical equations Eqs. (13-15).

In steady state, the atomic inversion is

$$\langle \hat{\sigma}_z^{(1)} \rangle = d_0 - \frac{2\Gamma_c(N-1)}{w + \Gamma_c} \langle \hat{\sigma}_+^{(1)} \hat{\sigma}_-^{(2)} \rangle. \quad (\text{A1})$$

Inserting that into Eq. (15) we end up with a linear equation for  $\langle \hat{\sigma}_z^{(1)} \hat{\sigma}_z^{(2)} \rangle$ . Solving that equation for  $\langle \hat{\sigma}_z^{(1)} \hat{\sigma}_z^{(2)} \rangle$  yields

$$\langle \hat{\sigma}_z^{(1)} \hat{\sigma}_z^{(2)} \rangle = d_0^2 + \frac{2\Gamma_c}{(w + \Gamma_c)^2} \left( (w + \Gamma_c)(1 - d_0(2N - 3)) + 2(N - 1)(N - 2)\Gamma_c \langle \hat{\sigma}_+^{(1)} \hat{\sigma}_-^{(2)} \rangle \right) \quad (\text{A2})$$

Inserting Eq. (A1) and Eq. (A2) into the remaining equation for  $\langle \hat{\sigma}_+^{(1)} \hat{\sigma}_-^{(2)} \rangle$  leads to a quadratic equation. One of the solutions must be discarded because it violates  $|\langle \hat{\sigma}_+^{(1)} \hat{\sigma}_-^{(2)} \rangle_c| \leq 1$  for certain repump rates and hence is unphysical. The physically acceptable solution is

$$\langle \hat{\sigma}_+^{(1)} \hat{\sigma}_-^{(2)} \rangle = -\frac{w + \Gamma_c}{4(N-1)(N-2)w\Gamma_c^2} \left[ w^2 + (2 - (N-2)d_0)w\Gamma_c + (N-1)(1+d_0)\Gamma_c^2 \right. \\ \left. - \sqrt{4d_0(1+d_0)(N-1)(N-2)w\Gamma_c^3 + (w^2 + (2 - (N-2)d_0)w\Gamma_c + (N-1)(1+d_0)\Gamma_c^2)^2} \right]. \quad (\text{A3})$$

This solution can then be inserted in Eq.(A1) and Eq.(A2) to find  $\langle \hat{\sigma}_z^{(1)} \rangle_c$  and  $\langle \hat{\sigma}_z^{(1)} \hat{\sigma}_z^{(2)} \rangle_c$ .

- 
- [1] F. Haake, H. King, G. Schröder, J. W. Haus, and R. J. Glauber, Phys. Rev. A **20**, 2047 (1979).
  - [2] J. P. Clemens and H. J. Carmichael, Phys. Rev. A **65**, 023815 (2002).
  - [3] F. Haake and J. W. Haus and H. King and G. Schröder and R. J. Glauber, Phys. Rev. A **23**, 1322 (1981).
  - [4] F. Haake, J. Haus, H. King, G. Schröder, and R. Glauber, Phys. Rev. Lett. **45**, 558 (1980).
  - [5] H. Uys, T. Miyakawa, D. Meiser, and P. Meystre, Phys. Rev. A **72**, 053616 (2005).
  - [6] R. Bonifacio, P. Schwendimann, and F. Haake, Phys. Rev. A **4**, 302 (1971).
  - [7] D. Meiser, J. Ye, D. R. Carlson, and M. J. Holland, Phys. Rev. Lett. **102**, 163601 (2009).
  - [8] D. Meiser and M. J. Holland (2009), 0912.0690.
  - [9] V. V. Temnov, Phys. Rev. A **71**, 053818 (2005).
  - [10] V. V. Temnov and U. Woggon, Phys. Rev. Lett. **95**, 243602 (2005).
  - [11] M. Scheibner, T. Schmidt, L. Worschech, A. Forchel, G. Bacher, T. Passow, and D. Hommel, Nature Physics **3**, 106 (2007).
  - [12] V. V. Temnov and U. Woggon, Opt. Express **17**, 5774 (2009).
  - [13] F. Haake, M. I. Kolobov, C. Fabre, E. Giacobino, and S. Reynaud, Phys. Rev. Lett. **71**, 995 (1993).
  - [14] F. Haake, M. I. Kolobov, C. Seeger, C. Fabre, E. Giacobino, and S. Reynaud, Phys. Rev. A **54**, 1625 (1996).
  - [15] J. Dalibard, Y. Castin, and K. Mølmer, Phys. Rev. Lett. **68**, 580 (1992).
  - [16] C. W. Gardiner, A. S. Parkins, and P. Zoller, Phys. Rev. A **46**, 4363 (1992).
  - [17] M. Plenio and P. Knight, Rev. Mod. Phys. **70**, 101 (1998).
  - [18] R. J. Glauber, Phys. Rev. **130**, 2529 (1963).
  - [19] L. Mandel and E. Wolf, *Optical Coherence and Quantum Optics* (Cambridge University Press, 1995).
  - [20] R. J. Glauber, Phys. Rev. **131**, 2766 (1963).
  - [21] C. W. Gardiner and P. Zoller, *Quantum Noise* (Springer, 2000).
  - [22] D. F. Walls and G. J. Milburn, *Quantum Optics* (Springer, 1994).
  - [23] G. Benivegna and A. Messina, Journal of Modern Optics **36**, 1205 (1989).
  - [24] S. Nicolosi, A. Napoli, and A. Messina, Eur. Phys. J. D **33**, 113 (2005).
  - [25] R. Loudon, *The Quantum Theory of Light* (Oxford Science Publications, 2003), 3rd ed.
  - [26] For simplicity we only consider the case of an even total number of atoms here. The argument applies with trivial modifications also to the case of an odd number of atoms.